© 2018. Published by The Company of Biologists Ltd | Development (2018) 145, dev156554. doi:10.1242/dev.156554

RESEARCH ARTICLE

NFIA and GATA3 are crucial regulators of embryonic articular cartilage differentiation

Pratik Narendra Pratap Singh[1,*], Upendra Singh Yadav[1], Kimi Azad[1,‡], Pooja Goswami[2], Veena Kinare[3] and Amitabha Bandyopadhyay[1,§]

ABSTRACT

During appendicular skeletal development, the bi-potential cartilage anlagen gives rise to transient cartilage, which is eventually replaced by bone, and to articular cartilage that caps the ends of individual skeletal elements. While the molecular mechanism that regulates transient cartilage differentiation is relatively well understood, the mechanism of articular cartilage differentiation has only begun to be unraveled. Furthermore, the molecules that coordinate the articular and transient cartilage differentiation processes are poorly understood. Here, we have characterized in chick the regulatory roles of two transcription factors, NFIA and GATA3, in articular cartilage differentiation, maintenance and the coordinated differentiation of articular and transient cartilage. Both NFIA and GATA3 block hypertrophic differentiation. Our results suggest that NFIA is not sufficient but necessary for articular cartilage differentiation. Ectopic activation of GATA3 promotes articular cartilage differentiation, whereas inhibition of GATA3 activity promotes transient cartilage differentiation at the expense of articular cartilage. We propose a novel transcriptional circuitry involved in embryonic articular cartilage differentiation, maintenance and its crosstalk with the transient cartilage differentiation program.

KEY WORDS: Articular cartilage, Interzone, Joint, Limb, Osteoarthritis, Transient cartilage, Chicken, Mouse

INTRODUCTION

Vertebrate limb skeletogenesis starts as a Sox9-positive mesenchymal condensation that undergoes differentiation to become Col2a1-expressing cartilage. Concomitant with cartilage differentiation, the anlagen is branched and segmented to give rise to most of the skeletal elements of the limb (Shubin and Alberch, 1986; Bi et al., 1999). Except for the cartilage on either side of the plane of segmentation, the rest of the cartilage in these elements is gradually replaced by bone. The cartilage that is replaced by bone is referred to as transient cartilage, while that which remains as cartilage is referred to as permanent or articular cartilage. The Col2a1-expressing chondrocytes present at the center of the cartilage primordium progressively differentiate into prehypertrophic chondrocytes, marked by *Ihh* expression, followed by maturation into collagen 10 (ColX)-expressing hypertrophic chondrocytes (Karsenty and Wagner, 2002; Archer et al., 2003; Kronenberg, 2003; Pacifici et al., 2005). Recently, our group has demonstrated that the nascent cartilage cells are bi-potential in nature and can give rise to transient or articular cartilage depending on their exposure to either BMP or Wnt signaling, respectively (Ray et al., 2015).

The interzone marks the site of the future joint. It is characterized morphologically by a region of densely packed flattened cells and molecularly by the presence of markers such as *Gdf5*, *Wnt9a* and *Enpp2* [autotaxin (*Atx*)], and the absence of the typical cartilage marker *Col2a1*. The interzone acts as a signaling center and is crucial for joint morphogenesis (Holder, 1977; Archer et al., 2003; Pacifici et al., 2005). Wnt ligands, secreted from the interzone, activate Wnt/β-catenin signaling in the cells immediately adjacent to the interzone and this is necessary for embryonic articular cartilage differentiation (Hartmann and Tabin, 2001; Guo et al., 2004; Später et al., 2006a,b; Ray et al., 2015). c-Jun is a crucial transcriptional activator of Wnt ligands, namely Wnt9a and Wnt16 (Kan and Tabin, 2013). Thus, to date, c-Jun, Wnt9a and β-catenin are the only molecules known to promote embryonic articular cartilage differentiation.

C-1-1, a chicken ERG variant, is the only reported joint-specific transcription factor capable of inhibiting or blocking maturation of transient cartilage into hypertrophic chondrocytes. It should, however, be noted that even though C-1-1 can inhibit transient cartilage differentiation, it has not been reported to induce the ectopic expression of articular cartilage markers other than tenascin C (Iwamoto et al., 2000, 2001, 2007).

Compared with other chondrocyte populations, our understanding of articular cartilage differentiation remains rudimentary despite tremendous progress in recent decades. For instance, we do not have a comprehensive knowledge of the transcription factors that are crucial for articular cartilage differentiation, nor do we know how articular cartilage evades hypertrophy and persists as permanent cartilage (Karsenty and Wagner, 2002). These are key aspects, as articular cartilage is the tissue that is affected, and suspected to undergo transient cartilage differentiation, in osteoarthritis, the most prevalent skeletal disease (Pitsillides and Beier, 2011).

Previously, we reported that the transcription factor *NFIA* is expressed in chick embryonic articular cartilage (Singh et al., 2016). Here, we identified another transcription factor, *GATA3*, to be expressed in chick embryonic articular cartilage. We performed gain- and loss-of-function studies for both NFIA and GATA3. Loss-of-function of NFIA resulted in a reduction of the interzone region, while that of GATA3 abrogated articular cartilage differentiation. Gain-of-function of both these molecules blocked hypertrophic cartilage differentiation, but only GATA3 can induce the ectopic expression of several articular cartilage markers. However, our

[1]Department of Biological Sciences and Bioengineering, Indian Institute of Technology, Kanpur, U.P. 208016, India. [2]Kalinga Institute of Industrial Technology, KIIT University, Bhubaneswar 751024, Odisha, India. [3]Department of Lifesciences, Sophia College for Women, Bhulabhai Desai Road, Mumbai 400026, India.
*Present address: Department of Medical Oncology and Center for Functional Cancer Epigenetics, Dana-Farber Cancer Institute, Boston, MA 02215, USA.
‡Present address: Kusuma School of Biological Sciences, Indian Institute of Technology Delhi, HauzKhas, New Delhi, Delhi 110016, India.

§Author for correspondence (abandopa@iitk.ac.in)

P.G., 0000-0003-3900-6947; V.K., 0000-0002-5089-5151; A.B., 0000-0002-0429-438X

Received 27 June 2017; Accepted 6 December 2017

Development (2018) 145, dev156554. doi:10.1242/dev.156554

results suggest that GATA3 needs to act in collaboration with other transcription factors for proper articular cartilage differentiation.

RESULTS

Knockdown of NFIA results in a reduced interzone domain

In a previous screen, we identified the transcription factor *NFIA* as expressed in the outer chondrogenic layers (OCLs) of developing chicken articular cartilage from HH28 to HH38 (Singh et al., 2016). In order to investigate the necessity of NFIA in articular cartilage differentiation, we downregulated endogenous NFIA expression utilizing a well-characterized RCAS-based shRNAi (cNFIA-RNAi) against chick *NFIA*. The specificity and efficacy of this construct in knocking down endogenous chick *NFIA* have been reported previously (Deneen et al., 2006). Embryonic chick limb buds were infected at HH14 with RCAS virus particles expressing cNFIA-RNAi and harvested at HH36 (Fig. S1, Materials and Methods). Knockdown of NFIA resulted in micromelia of the infected limbs (Fig. S2C,D), as compared with the uninfected contralateral limbs (Fig. S2A,B). Skeletal preparation analysis of cNFIA-RNAi-infected limbs revealed shortening of the elements and unsegmented phalangeal elements (Fig. S2D′, arrows mark the unsegmented joints), as compared with the uninfected contralateral control (Fig. S2B,B′, arrow marks a segmented joint).

For molecular analysis, the region and extent of infection were assessed by immunohistochemistry against one of the viral gag proteins using 3C2 antibody (Fig. 1A). In the uninfected contralateral control joints the chick interzone is visualized as a *COL2A1*-negative, three-layered structure comprising a central intermediate layer (IL) flanked by two OCLs (Fig. 1B,B′, dotted lines). The presence of such an organized three-layered interzone could not be visualized in cNFIA-RNAi-infected joints (Fig. 1E,E′). Moreover, knockdown of NFIA resulted in a reduction in the *COL2A1*-negative interzone (compare red line in Fig. 1B,E).

Furthermore, analysis of layer-specific markers by RNA *in situ* hybridization revealed loss of both the outer and intermediate layers of the interzone following knockdown of NFIA, as demonstrated by downregulation of the IL marker *PHLDA2* and OCL marker *ChEST302p20* (compare Fig. 1C,C′ with F,F′, and D,D′ with G,G′). In extreme cases, complete loss of the *COL2A1*-negative domain

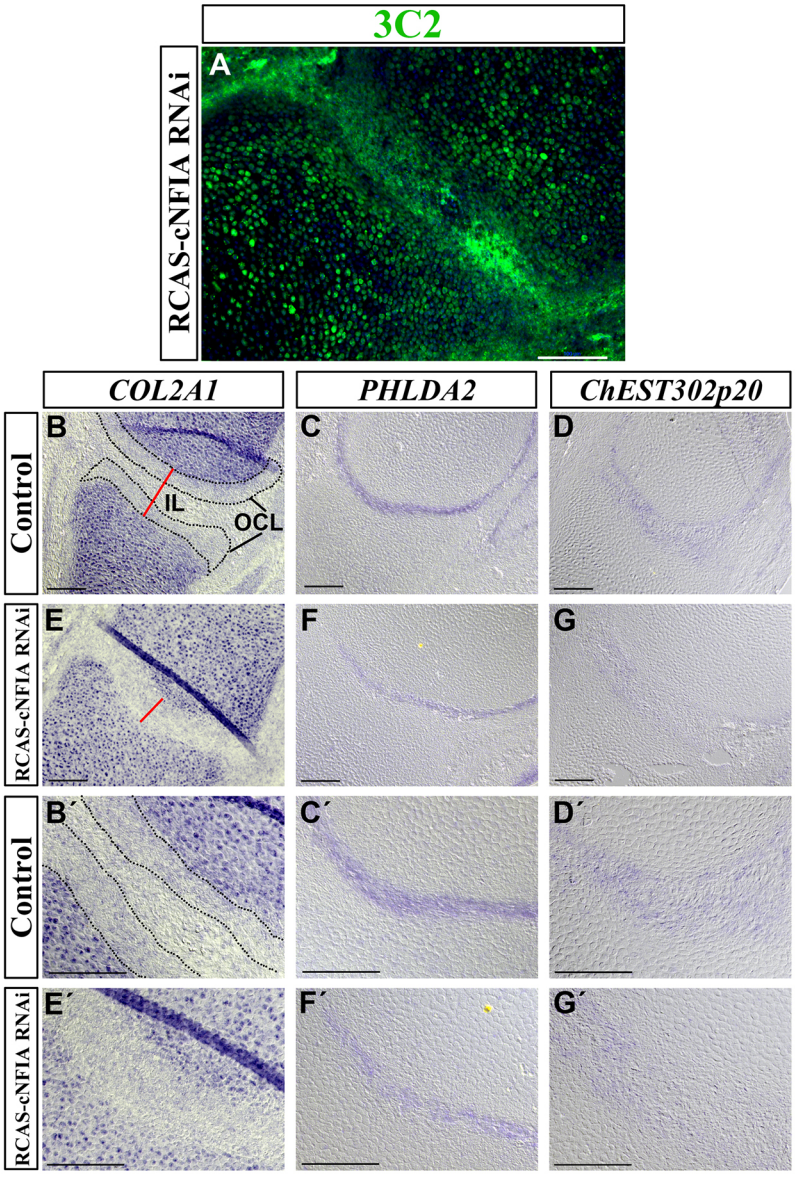

Fig. 1. NFIA loss-of-function leads to a reduction in interzone thickness. (A) Immunohistochemistry with 3C2 (antibody against the viral gag protein) marks the viral infection domain (green) in HH36 chick embryos. (B-G′) RNA *in situ* hybridization for *COL2A1*, *PHLDA2* and *ChEST302p20* in the (B-D) metatarsophalangeal (MTP) joint of the uninfected contralateral control limb and (E-G) RCAS-cNFIA RNAi-infected MTP joint region. (B′-G′) Magnified regions from B-G. Dotted lines (B,B′) mark the outer chondrogenic layers (OCLs) and sandwiched between them is the intermediate layer (IL). A,E-G and B-D are serial sections separated by 5 µm. *n*=5. Scale bars: 100 µm.

Development (2018) 145, dev156554. doi:10.1242/dev.156554

across some of the infected tibia-tarsus joint was observed (Fig. S3A,A′).

While analyzing the expression of *COL2A1* transcripts in cNFIA-RNAi-infected elements we noticed that the downregulation of *COL2A1* expression at the center of the elements (Fig. 2A, arrows), which is typically associated with the onset of hypertrophic differentiation, did not take place (compare Fig. 2A,A′). Thus, we investigated the status of hypertrophic differentiation in cNFIA-RNAi-infected elements. RNA *in situ* hybridization revealed that *IHH* expression was not downregulated at the center of the element, the putative hypertrophic region (Fig. 2B,B′, yellow and red arrowheads). ColX immunoreactivity could not be detected in cNFIA-RNAi-infected elements (Fig. 2D,D′, yellow and red arrowheads). Since PTHrP-PTHrPR signaling plays a crucial role in hypertrophic differentiation (Kronenberg, 2003), we investigated the mRNA expression of *PTHrP* and *PTHrPR*. We could not detect any variation in *PTHrP* expression (data not shown) but expression of *PTHrPR* was clearly downregulated in cNFIA-RNAi-infected elements (Fig. 2C,C′, yellow and red arrowheads).

NFIA gain-of-function promotes chondrogenesis

Next, to assess whether NFIA gain-of-function can promote an ectopic or expanded articular cartilage domain, HH14 chick limb buds were infected with RCAS retroviral particles expressing mouse *Nfia* cDNA (m*Nfia*). The embryos were harvested at HH36. Expression of RCAS-m*Nfia* resulted in micromelia of the infected limbs (Fig. S2E,G) and skeletal preparation analysis revealed a decrease in Alizarin Red staining (Fig. S2H′, asterisk), along with shortened and unsegmented skeletal elements (Fig. S2H,H′, arrows), as compared with uninfected contralateral control limb (Fig. S2F,F′).

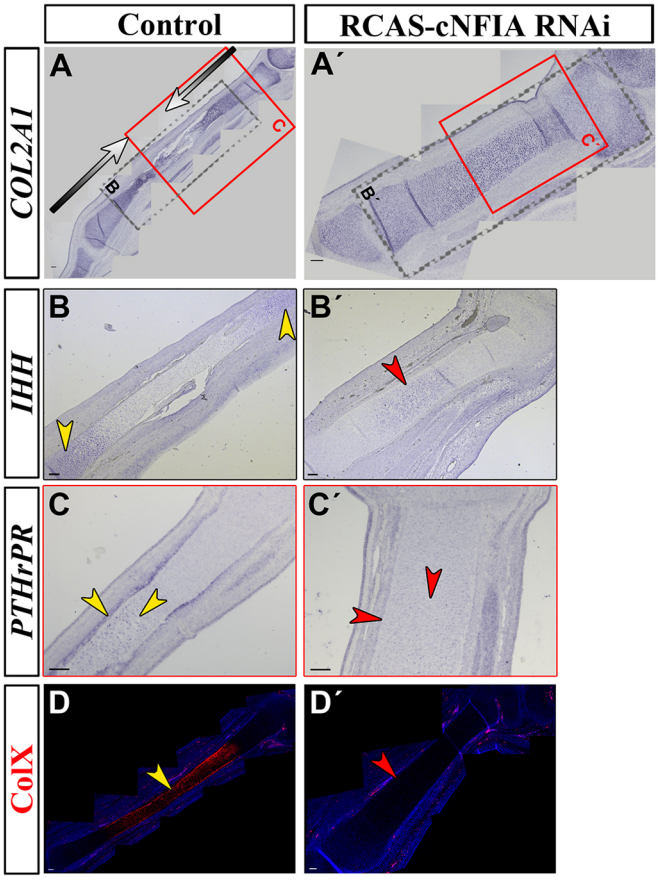

Fig. 2. NFIA loss-of-function blocks the progression of transient cartilage differentiation. (A-D) Tibia of uninfected contralateral control limb and (A′-D′) RCAS-cNFIA RNAi-infected tibia element at HH36. RNA *in situ* hybridization for *COL2A1* (A,A′), *IHH* (B,B′) and *PTHrPR* (C,C′), and immunohistochemistry for ColX (D,D′). Arrows (A) indicate the graded expression of *COL2A1* which is missing in A′. Yellow arrowheads (B-D) mark expression domains of *IHH*, *PTHrPR* and ColX, while red arrowheads (B′-D′) mark their downregulation in RCAS-cNFIA RNAi. *n*=5. Scale bars: 100 µm.

To assess molecular changes caused by m*Nfia* expression, we harvested RCAS-m*Nfia*-infected as well as uninfected contralateral control limbs. The region of infection within cartilage was assessed by (1) expression of m*Nfia* transcripts (Fig. 3A′) and (2) 3C2 immunoreactivity (Fig. 3H″). In agreement with observations of unsegmented skeletal elements (Fig. S2H′), we found that upon m*Nfia* infection the expression of several articular cartilage/interzone-specific markers, such as *GDF5*, *BMP4* and *SFRP2*, was downregulated (Fig. 3B-D′) in the putative joint region (Fig. 3B′-D′, black arrows). Thus, contrary to our expectation, we could not detect ectopic expression of any of the articular cartilage markers in the infected cells.

It should also be noted that, upon m*Nfia* expression, the cells of the putative interzone region often assumed a rounded morphology akin to cells in the epiphysis region (Fig. 3E′, black arrow) as opposed to the densely packed flattened morphology characteristic of interzone cells (Fig. 3E). These molecular and histological changes were particularly apparent in the phalangeal joints, as opposed to more proximal joints. Moreover, these RCAS-m*Nfia*-infected cells also expressed the early transient cartilage marker *COL2A1* (Fig. 3F,F′). The cell-autonomous effect of m*Nfia* expression is best exemplified in a joint that is partially infected. In such a joint, in the region that remained uninfected the articular chondrocytes not only maintained their densely packed flattened morphology (Fig. 3E′, red arrow) but also were *COL2A1* negative (Fig. 3F′, red arrow), whereas the adjoining infected interzone cells (Fig. 3A′, black arrow) adopted transient cartilage-like morphology (Fig. 3E′, black arrow) and expressed *COL2A1* (Fig. 3F′, black arrow).

The interzone or developing articular cartilage is largely non-proliferative, in contrast to adjacent transient cartilage cells (Ray et al., 2015). As expression of m*Nfia* led to downregulation of several articular cartilage markers and to ectopic expression of *COL2A1*, we determined the status of BMP signaling and cell proliferation in RCAS-m*Nfia*-infected putative interzone cells. We carried out immunohistochemistry for pSMAD1/5/8, as a readout of BMP signaling, and for the mitotic marker phosphohistone H3 (pH3). As expected, we could detect ectopic pSMAD1/5/8 immunoreactivity (Fig. 3G-G″) along with phosphohistone H3 (Fig. 3H,H′) in putative joint sites in m*Nfia*-infected tissues (3C2 immunostaining in Fig. 3H″).

NFIA gain-of-function blocks chondrocyte differentiation into the prehypertrophic state, maintaining a stable immature state

Skeletal analysis of m*Nfia*-infected limbs revealed a decrease in Alizarin Red staining (Fig. S2H,H′). Therefore, we investigated the molecular changes associated with endochondral ossification. Expression of *COL2A1* transcripts, which is normally reduced upon onset of hypertrophy, did not decrease from the epiphysis to the diaphysis of RCAS-m*Nfia*-infected cartilage elements (Fig. 4A,A′).

In keeping with this, analysis of *IHH* and ColX expression revealed that expression of m*Nfia* blocked prehypertrophic chondrocyte differentiation. There was a marked decrease in the expression of

Development (2018) 145, dev156554. doi:10.1242/dev.156554

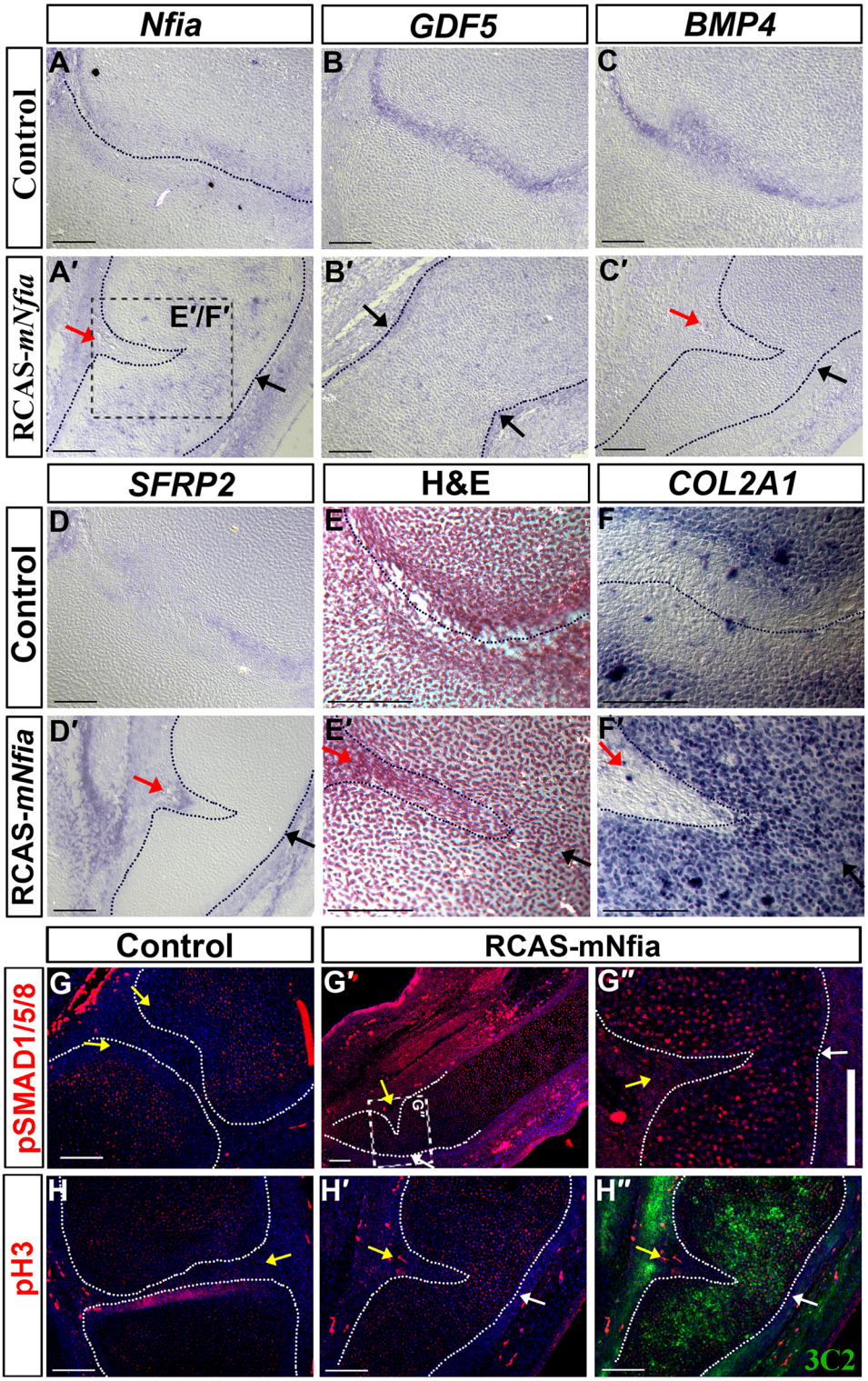

Fig. 3. NFIA gain-of-function leads to loss of the putative joint site and induces chondrogenesis. (A-H) MTP joint of the uninfected contralateral control limb and (A′-H′) RCAS-m*Nfia*-infected MTP joint region at HH36. RNA *in situ* hybridization for m*Nfia* (A,A′), *GDF5* (B,B′), *BMP4* (C,C′), *SFRP2* (D,D′) and *COL2A1* (F,F′), and Hematoxylin and Eosin staining (E,E′). (A′-F′) Black arrows mark the absence of a putative MTP joint region due to RCAS-m*Nfia* infection, while red arrows mark the uninfected MTP joint region within the same element. Immunohistochemistry for (G-G″) pSMAD1/5/8 and (H,H′) phosphohistone H3. (H′′) Overlap of infected region (3C2, green) and pH3 immunoreactivity from H′. (G′-H″) White arrows mark the absence of a putative MTP joint region due to RCAS-m*Nfia* infection, while yellow arrows mark the uninfected MTP joint region within the same element. In the uninfected contralateral control, yellow arrows mark the absence of pSMAD1/5/8 within the interzone and in the adjacent domain (G), and the phosphohistone H3-negative interzone region (H). Skeletal elements are outlined with dotted lines. Serial sections (except B′) separated by 5 µm. *n*=6. Scale bars: 100 µm.

IHH transcripts (Fig. 4B′) and ColX protein (Fig. 4C′) in the infected transient cartilage cells as compared with the uninfected contralateral cartilage element (Fig. 4B-C′). Thus, although RCAS-m*Nfia*-infected cells continued to express *COL2A1* they did not progress further in the transient cartilage differentiation program and were arrested in an initial chondrogenic state.

Several lines of investigation have demonstrated that both Ihh and Pthrp block hypertrophic differentiation of cartilage and that IHH can induce expression of *PTHrP* in the periarticular region through a long-range negative-feedback loop (Lanske et al., 1996; Vortkamp et al., 1996; St-Jacques et al., 1999; Dentice et al., 2005; Koziel et al., 2005). Thus, we hypothesized that expression of m*Nfia* might be affecting this IHH/PTHrP regulatory loop. We analyzed the expression pattern of PTHrP in m*Nfia*-expressing chick limbs. As expected, loss of *IHH* resulted in reduced expression of *PTHrP* in RCAS-m*Nfia*-infected joints (Fig. 4D,D′, black arrow).

Development (2018) 145, dev156554. doi:10.1242/dev.156554

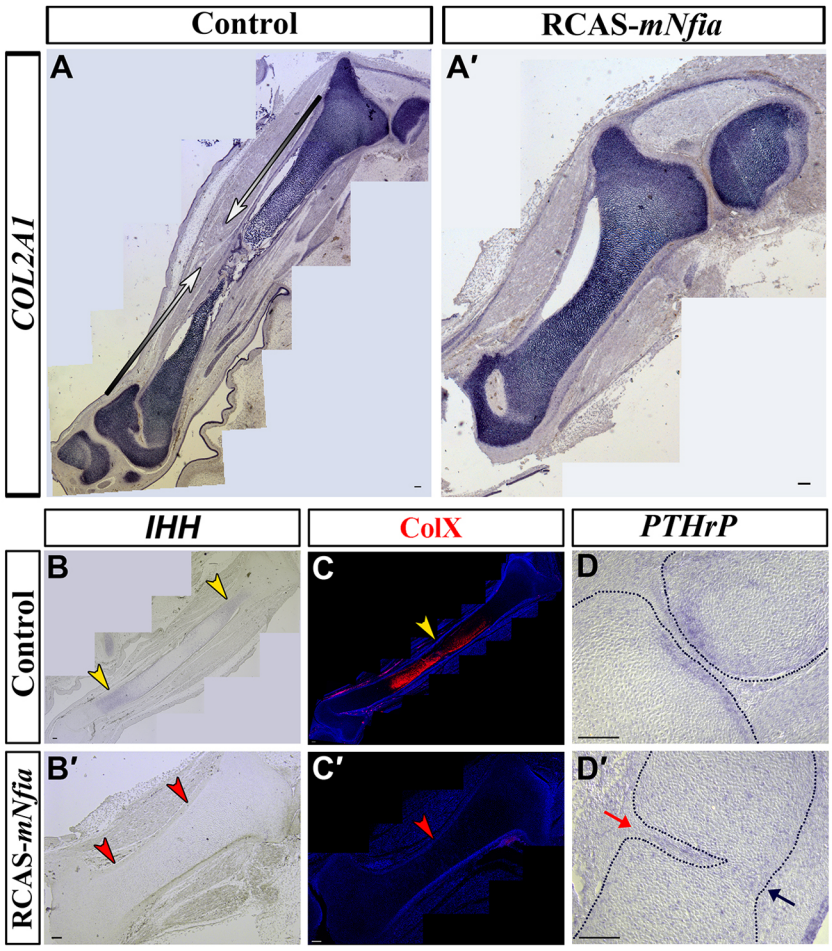

Fig. 4. NFIA gain-of-function blocks maturation of transient cartilage cells into prehypertrophy and hypertrophy. (A-C) Tibia of uninfected contralateral control limb and (A′-C′) RCAS-m*Nfia*-infected tibia element at HH36. (D) MTP joint region of uninfected contralateral control and (D′) RCAS-m*Nfia*-infected MTP joint at HH36. RNA *in situ* hybridization for *COL2A1* (A,A′), *IHH* (B,B′) and *PTHrP* (D,D′), and immunohistochemistry for ColX (C,C′). Red arrows (A) mark gradual downregulation of *COL2A1* expression from epiphysis to diaphysis as the chondrocytes undergo maturation, which is not apparent in the RCAS-m*Nfia*-infected tibia element (A′). Yellow arrowheads mark the region of *IHH* (B) and ColX (C) expression in control, while red arrowheads mark the absence of *IHH* (B′) and of ColX (C′) expression in the RCAS-m*Nfia*-infected tibia element. (D,D′) Skeletal element is outlined by dotted lines; the black arrow marks the RCAS-m*Nfia*-infected putative MTP joint region, while the red arrow marks the uninfected MTP joint region within the same element. A-C and A′-C′ are serial section images separated by 5 µm. (D,D′) Serial sections of the specimen used in Fig. 3A′-H′, except B′. *n*=6. Scale bars: 100 µm.

Identification of *GATA3* as an articular cartilage-specific gene and generation of GATA3 loss-of-function constructs

Bonilla-Claudio et al. (2012) recently reported *Gata3* to be a direct transcriptional target of BMP signaling during intramembranous ossification. While investigating whether *GATA3* is also expressed during endochondral ossification in a BMP signaling-dependent manner, we discovered that *GATA3* is in fact expressed specifically in the developing articular cartilage/interzone of chick (Fig. 5A-E) and mouse (Fig. S6A,A′). Further, *Gata3* has been suggested to promote the expression of 16 genes that are expressed in the articular cartilage (Table S1) in a previous microarray transcriptomic profiling of whole mammary glands (Kouros-Mehr et al., 2006). Thus, *GATA3* was an obvious candidate for a possible role in inducing articular cartilage fate.

In order to study the effects of loss-of-function of GATA3 with respect to chicken embryonic articular cartilage development, we created a dominant-negative version of GATA3 following the strategy of Kamei et al. (2011). Alignment of the amino acid sequences of the chick and mouse GATA3 DNA-binding domains reveals a sequence identity of 100%. Therefore, in order to generate a dominant-negative form of GATA3, we fused the DNA-binding domain of mouse *Gata3* to the Engrailed transcriptional repressor domain (m*Gata3*-EnR) (Fig. S4C).

GATA3 loss-of-function results in the absence of joint and downregulation of articular cartilage markers

The existing data indicating that loss of *Gata3* expression is associated with the downregulation of expression of 16 articular cartilage markers (Kouros-Mehr et al., 2006) (Table S1) suggested that Gata3 plays an instructive role in articular cartilage differentiation. To investigate whether GATA3 is necessary for chick articular cartilage development we expressed m*Gata3*-EnR in the prospective limb field by electroporation of the RCAS-m*Gata3*-EnR construct at HH14. The efficiency of electroporation was assessed by co-electroporating a pCAG-mCherry reporter construct (Fig. S1, Materials and Methods). The embryos were harvested at HH36. Electroporation of embryonic limb buds with RCAS-m*Gata3*-EnR consistently resulted in digit truncation and interdigital syndactyly (Fig. S5C). In extreme cases, we also observed hemangioma/blood pooling at the distal end of an infected limb (Fig. S5B). Whole-mount skeletons of RCAS-m*Gata3*-EnR-electroporated limbs stained with Alcian Blue and Alizarin Red revealed a decrease in Alizarin Red staining (Fig. S5B′, asterisks) along with unsegmented skeletal elements (Fig. S5C′, arrows), as compared with the uninfected contralateral control (Fig. S5A,A′).

To analyze molecular and histological changes brought about by GATA3 loss-of-function, we analyzed sections of m*Gata3*-EnR-infected limbs. The region of infection within cartilage was assessed by expression of m*Gata3* mRNA (Fig. 5J′) and by 3C2 immunoreactivity (Fig. 5L″,L‴). Expression of the dominant-negative m*Gata3*-EnR resulted in ectopic expression of the transient cartilage marker *COL2A1* (Fig. 5F,F′) and the absence of joint-specific markers *SFRP2*, *ENPP2* and *GDF5* (Fig. 5G-I′) in the putative joint region cells (black arrows).

Moreover, we observed that m*Gata3*-EnR-infected interzone cells are mitotically active, as assessed by pH3 immunoreactivity (Fig. 5L,L′), and are pSMAD1/5/8 positive (Fig. 5K,K′), thus

Development (2018) 145, dev156554. doi:10.1242/dev.156554

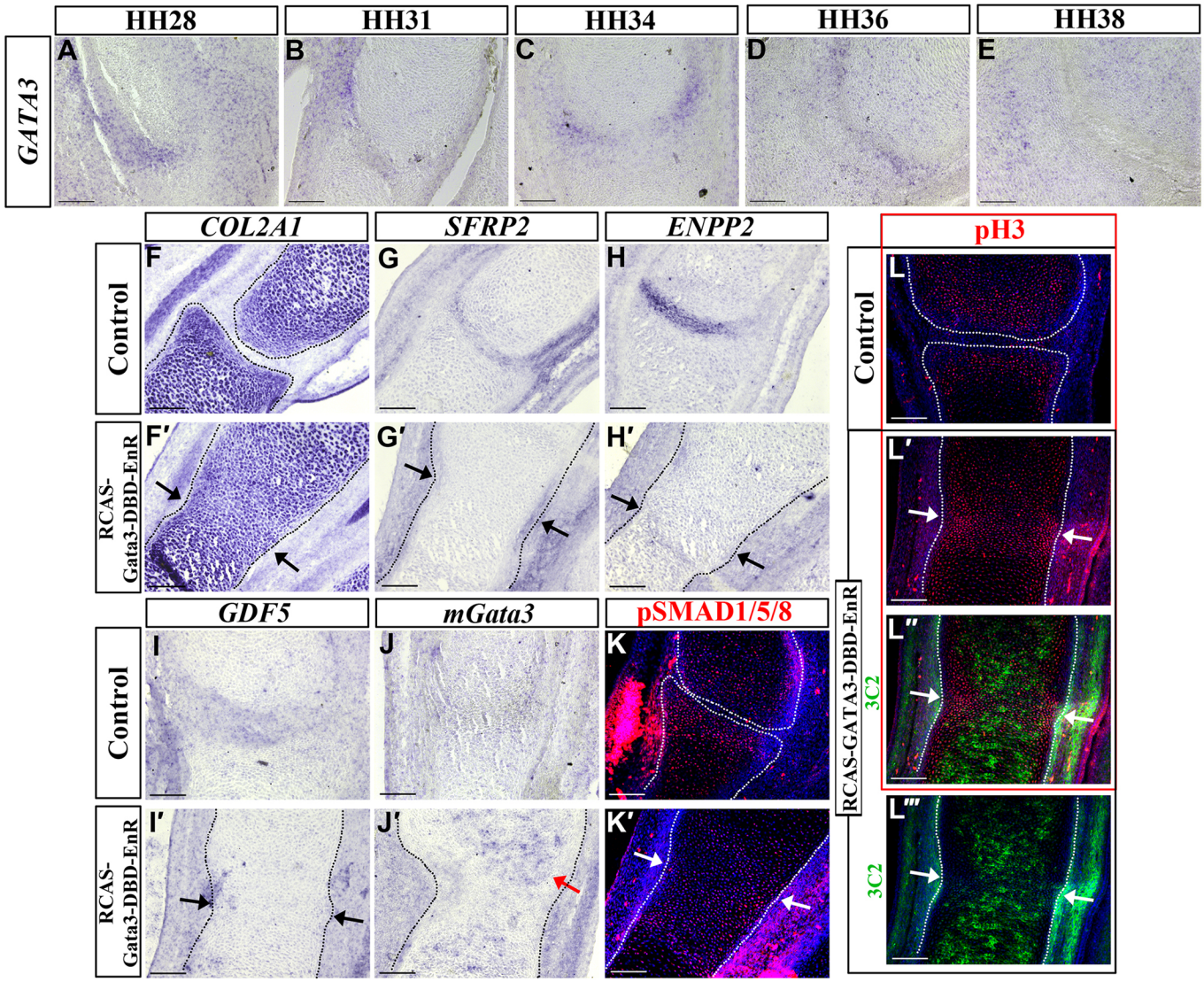

Fig. 5. GATA3 loss-of-function leads to loss of the putative joint site and induces transient cartilage-like fate in the putative joint region. (A-E) RNA *in situ* hybridization for *GATA3* in chick MTP joint from HH28-HH38. (F-L) MTP joint of the uninfected contralateral control limb and (F′-L′) RCAS-m*Gata3*-EnR-infected MTP joint region. RNA *in situ* hybridization for *COL2A1* (F,F′), *SFRP2* (G,G′), *ENPP2* (H,H′), *GDF5* (I,I′) and m*Gata3* (J,J′). Black arrows mark the absence of the putative phalangeal joint region due to RCAS-m*Gata3*-EnR infection. Red arrow (J′) marks the expression of m*Gata3* across the putative phalangeal joint region. Immunohistochemistry for pSMAD1/5/8 (K,K′), phosphohistone H3 (L,L′) and 3C2 (antibody against viral gag protein) (L‴). (L″) Merge of L′ and L‴. White arrows mark the loss of the putative phalangeal joint region due to RCAS-m*Gata3*-EnR infection. F′-H′,K′ and I′,J′,L′ are serial sections separated by 5 µm. *n*=7. Scale bars: 100 µm.

mimicking the attributes of transient cartilage. It should be noted that in m*Gata3*-EnR-expressing limbs, normal hypertrophic differentiation was unaffected (data not shown).

GATA3 gain-of-function results in the appearance of ectopic articular cartilage markers

Having established that GATA3 loss-of-function results in downregulation of several articular cartilage markers, we next asked whether misexpression of *GATA3* could promote an ectopic or expanded domain of articular cartilage markers. To investigate this, we expressed m*Gata3* cDNA in HH14 limb buds (RCAS-m*Gata3*) and harvested the embryos at HH36. Expression of m*Gata3* in limb buds did not result in any gross phenotype apparent in the whole mount (data not shown). Thus, we used pCAG-mCherry as an electroporation marker and analyzed limb buds that were efficiently electroporated. We generated sections from these limbs and analyzed for molecular changes. Regions of infection within sections of limb cartilage were assessed by m*Gata3* RNA *in situ* hybridization (Fig. 6A′). Analysis of articular cartilage-specific markers revealed mild ectopic expression of *c-JUN* and *WNT9A* mRNAs within the domains of m*Gata3* expression (Fig. 6B-C′). We also observed weak ectopic β-catenin immunoreactivity in cells surrounding the ectopic domains of *c-JUN* and *WNT9A* expression (Fig. 6D,D′). Although expression of m*Gata3* resulted in the ectopic expression of *c-JUN* and *WNT9A*, it did not stimulate the ectopic expression of many other articular cartilage markers (Fig. S6B-F).

We speculated that GATA3 alone might not be sufficient to promote articular cartilage differentiation and that it needs other transcriptional collaborators. To investigate this possibility we fused the DNA-binding domain of mGata3 to the VP16 transcriptional activator domain (m*Gata3*-VP16) (Fig. S4B) (Kamei et al., 2011).

Development (2018) 145, dev156554. doi:10.1242/dev.156554

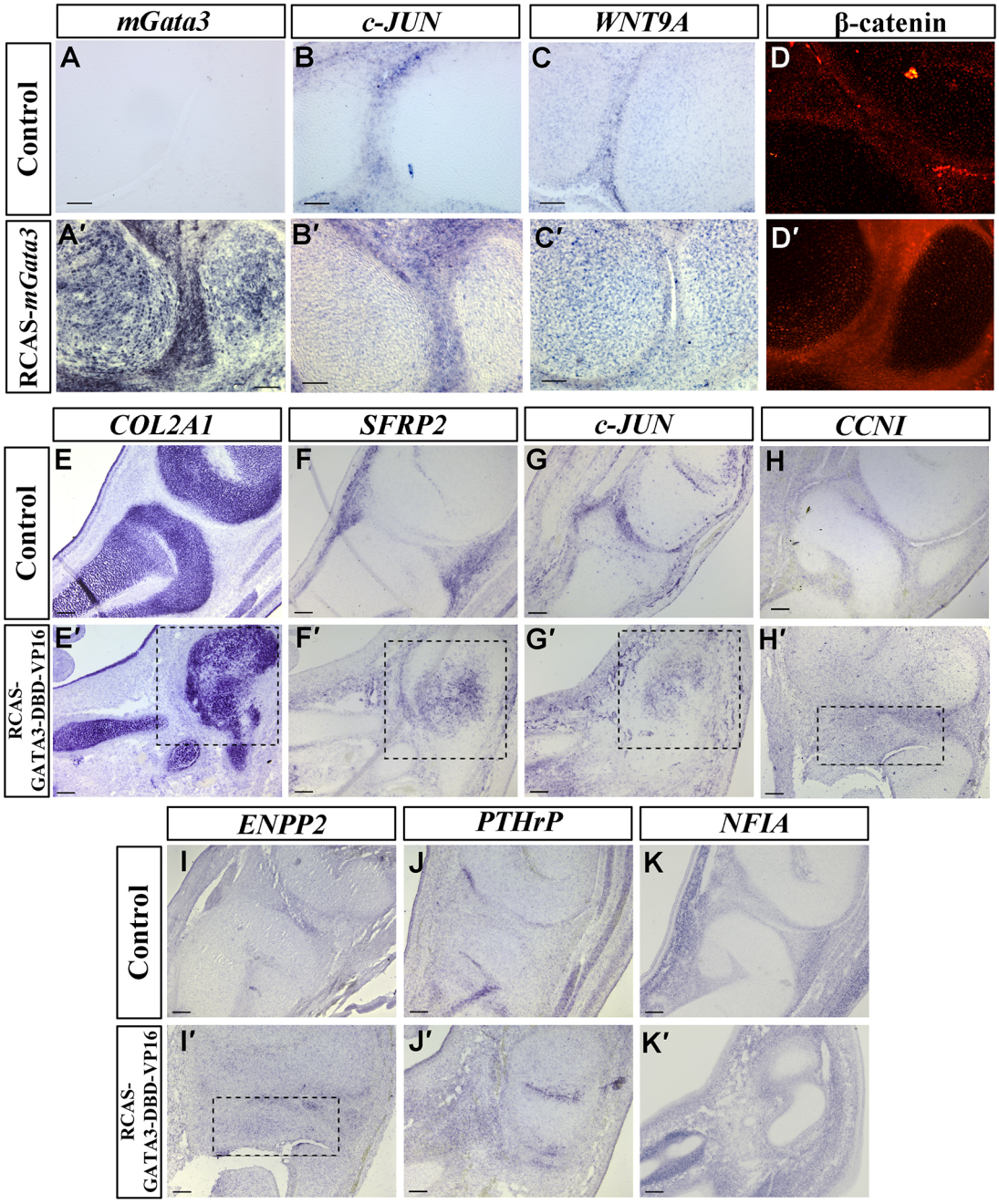

Fig. 6. GATA3 gain-of-function promotes ectopic expression of articular cartilage markers. (A-D) Tibio-tarsal joint of an uninfected contralateral control limb and (A′-D′) RCAS-m*Gata3*-infected tibio-tarsal joint region. RNA *in situ* hybridization for m*Gata3* (A,A′), *c-JUN* (B,B′), *WNT9A* (C,C′), and immunohistochemistry for β-catenin (D,D′). (E-K) Tibio-tarsal joint of an uninfected contralateral control limb and (E′-K′) RCAS-m*Gata3*-VP16-infected tibio-tarsal joint region showing RNA *in situ* hybridization for the indicated genes. Dotted boxes outline (E′-G′) the downregulation of *COL2A1* along with the ectopic expression of *SFRP2* and *c-JUN* in similar regions, or (H′-I′) the ectopic expression of *CCNI* and *ENPP2* in similar regions. E′-G′,J′-K′ and H′,I′ are serial sections separated by 5 µm. For RCAS-m*Gata3*, *n*=4; for RCAS-m*Gata3*-VP16, *n*=6. Scale bars: 100 µm.

Such fusion proteins are directed to their cognate binding sites in enhancers by the DNA-binding domain, whereupon they activate transcription under the control of the enhancer irrespective of the presence of co-factors, and thus act as a constitutively active version of the transcription factor.

We introduced the RCAS-m*Gata3*-VP16 construct into HH14 limb buds and harvested the embryos at HH36. Inspection of freshly harvested unfixed, unstained, RCAS-m*Gata3*-VP16-infected limbs revealed micromelia (shortened limb elements), interdigital syndactyly and hematoma/hemorrhage (Fig. S5E), as compared with the uninfected contralateral control limb (Fig. S5D). Whole-mount skeletons of RCAS-m*Gata3*-VP16-infected limbs stained with Alcian Blue and Alizarin Red revealed a decrease in Alizarin Red staining along with shortened, unsegmented skeletal elements (Fig. S5E′), compared with the uninfected contralateral control (Fig. S5D′).

The region of infection within sections of limb cartilage was assessed by 3C2 immunoreactivity (Fig. 7A″-C″). Expression of constitutively active m*Gata3* resulted in the ectopic expression of four joint-specific markers, namely *SFRP2*, *c-JUN*, *CCNI* and

Development (2018) 145, dev156554. doi:10.1242/dev.156554

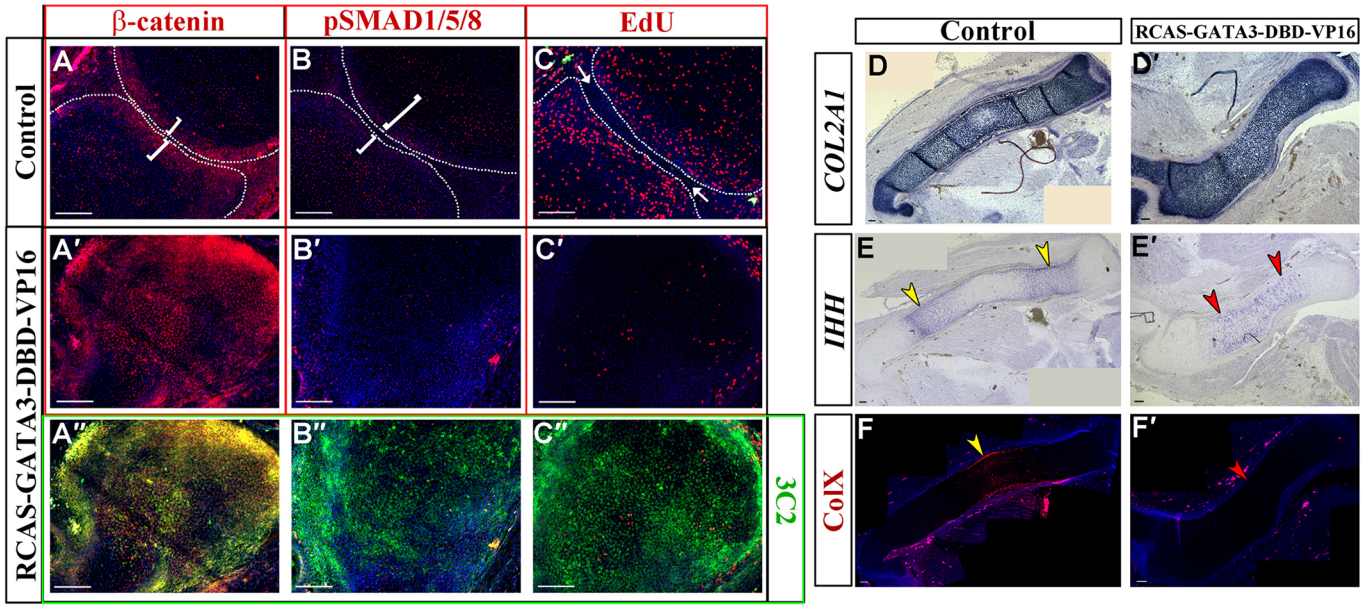

Fig. 7. GATA3 gain-of-function induces articular cartilage-like attributes in putative transient cartilage cells and blocks maturation of transient cartilage cells to the hypertrophic state. (A-C) Tibio-tarsal joint of the uninfected contralateral control limb and (A′-C′) RCAS-m*Gata3*-VP16-infected tibio-tarsal joint region. Immunohistochemistry for (A,A′) β-catenin or (B,B′) pSMAD1/5/8. (C,C′) EdU-incorporated cells are in red. (A″-C″) Double immunohistochemistry with anti-β-catenin (A″), anti-pSMAD1/5/8 (B″) and EdU-incorporated cells (C″) in red and 3C2 (antibody against viral gag protein) in green. (A′-C′) Magnified images of a similar region to that indicated by the dotted boxed in Fig. 6E′-G′; serial section images separated by 5 µm. Dotted lines delineate the interzone region. Square brackets mark the chondrogenic layers adjacent to the joint line that are positive for β-catenin but negative for pSMAD1/5/8. Arrows indicate the joint line deficient in proliferative cells. (D-F) Femur of uninfected contralateral control limb and (D′-F′) RCAS-m*Gata3*-VP16-infected femur, showing RNA *in situ* hybridization for *COL2A1* (D,D′) and *IHH* (E,E′), and immunohistochemistry for ColX (F,F′). D-F and D′-F′ are serial section images separated by 5 µm. Yellow arrowheads (E,F) mark expression domains of *IHH* and ColX, while red arrowheads (E′,F′) mark their downregulation in RCAS-m*Gata3*-VP16. For RCAS-m*Gata3*-VP16, *n*=6. Scale bars: 100 µm.

ENPP2 (dotted box, Fig. 6F-I′). Despite the rather broad domains of m*Gata3*-VP16 expression, ectopic expression of joint-specific markers was present only near the putative joint site. The expression of some of the other articular cartilage markers, such as *PTHrP*, *NFIA*, *PHLDA2* and *ChEST302p20*, remained unaltered (Fig. 6J-K′; data not shown). The ectopic expression of articular cartilage markers was accompanied with a slight downregulation of *COL2A1*, a transient cartilage marker, in the m*Gata3*-VP16-infected cells near the future joint region (Fig. 6E,E′).

As stated above, previous analyses have shown that, in contrast to transient cartilage, articular cartilage cells are largely non-proliferative, β-catenin positive and pSMAD1/5/8 negative (Ray et al., 2015). We wanted to assess whether the m*Gata3*-VP16-infected putative transient cartilage cells, which expressed ectopic articular cartilage markers, also attained these attributes of articular cartilage. To assess proliferation, we labeled the dividing cells in the embryo with EdU, a thymidine analog. Akin to articular cartilage cells in the contralateral limb (the region indicated by arrows between dotted lines, Fig. 7C), the number of EdU-positive cells was reduced in m*Gata3*-VP16-infected cells (Fig. 7C′,C″) and, moreover, this was accompanied by ectopic induction of *WNT9A* (Fig. S6G-J) and β-catenin (Fig. 7A,A′) along with downregulation of pSMAD1/5/8 (Fig. 7B,B′). Overall, these lines of evidence suggest that GATA3 gain-of-function promotes articular cartilage fate at the expense of transient cartilage.

GATA3 gain-of-function blocks chondrocyte differentiation from the prehypertrophic to hypertrophic state

In an uninfected contralateral control cartilage anlagen, *COL2A1* expression gradually decreases from the epiphysis towards the center of the cartilage element where hypertrophic differentiation takes place (Fig. 7D). Expression of constitutively active m*Gata3* blocks such downregulation of *COL2A1* expression (Fig. 7D′). Furthermore, m*Gata3*-VP16 arrested the chondrocytes in a prehypertrophic state, as marked by a contiguous band of *IHH*-expressing cells within the center of the cartilage element (Fig. 7E′, arrows) and blocked further transition to the hypertrophic state as demonstrated by the absence of ColX (Fig. 7F′, arrow); by contrast, in the control, *IHH* was expressed as two discrete bands (Fig. 7E, arrows) with ColX expressed in the center (Fig. 7F, arrow). These observations are somewhat similar to what was observed in NFIA loss-of-function limbs (compare Fig. 2A,B,D and A′,B′,D′). It should however be noted that although m*Gata3*-VP16 was expressed even in the prehypertrophic region, the articular cartilage markers were not ectopically expressed in these domains.

DISCUSSION

Transcriptional regulation of articular cartilage differentiation and maintenance is not well understood. Previously, we reported the identification of *NFIA* as an articular cartilage-specific transcription factor (Singh et al., 2016). In the present report, we identified *GATA3* as another transcription factor that is specifically expressed in chick and mouse articular cartilage, and characterized the roles of NFIA and GATA3 during chick articular cartilage differentiation. Our data suggest that although NFIA is not sufficient for articular cartilage differentiation, it is necessary to maintain the permanent fate of articular cartilage through prevention of hypertrophic differentiation. Gain- and loss-of-function experiments demonstrated that GATA3 is necessary for articular cartilage differentiation and for this requires the cooperation of other, unknown activation factors.

Development (2018) 145, dev156554. doi:10.1242/dev.156554

Role of NFIA in joint development

Knockdown of chick NFIA reduces or abolishes the *COL2A1*-negative interzone domain, while misexpression of NFIA prevents hypertrophic differentiation of the transient cartilage cells. Taken together, it appears that NFIA primarily aids in the maintenance of articular cartilage fate by preventing hypertrophic differentiation of interzone/articular cartilage cells.

Nfia is expressed specifically in E16.5 mouse articular cartilage (Fig. S3C,C′). However, in contrast to the effects of knockdown of NFIA in chick embryos, disruption of the *Nfia* gene in mice did not result in a dramatic phenotype, with only a mild disruption of the organization of articular cartilage (Fig. S3E-H′). This rather mild morphological defect in skeletal and cartilage elements might be due to redundancy (das Neves et al., 1999). Indeed, *Nfia* has several homologs, including *Nfib*, *Nfic* and *Nfix*, and we also detected expression of *Nfix* in mouse articular cartilage (Fig. S3D,D′). It will be interesting to analyze the effects of compound knockouts of combinations of these factors in articular cartilage differentiation.

Expression of m*Nfia* in the developing chick limb skeleton promoted ectopic expression of *COL2A1* transcripts in the putative interzone/articular cartilage cells. This is paradoxical considering that embryonic articular cartilage does not normally express *Col2a1* mRNA. It should be noted that although some of the articular cartilage-specific genes, such as *Wnt9a*, *Wnt4* and *Wnt16*, are anti-chondrogenic in nature, there are others, such as *Gdf5* and *Gdf6*, which are chondrogenic. Ectopic chondrogenesis and abrogation of articular joint formation upon overexpression of NFIA is very similar to what is observed with GDF5 overexpression (Francis-West et al., 1999; Merino et al., 1999; Storm and Kingsley, 1999; Tsumaki et al., 1999). However, Gdf5 misexpression is not reported to cause a block in hypertrophy. C-1-1 was proposed to be a Gdf5 target and its misexpression causes a block in hypertrophy similar to that which we observe with NFIA misexpression, but the effect of C-1-1 misexpression on ectopic chondrogenesis (ectopic *Col2a1* expression) has not been reported (Iwamoto et al., 2001, 2000). Finally, just like NFIA, both gain- and loss-of-function manipulations of GDF5 cause abrogation of joint formation. The broad similarity in articular cartilage developmental defects upon gain- or loss-of-function manipulations of GDF5, ERG or NFIA raises the question as to whether these genes functionally interact during normal articular cartilage development (Fig. 8).

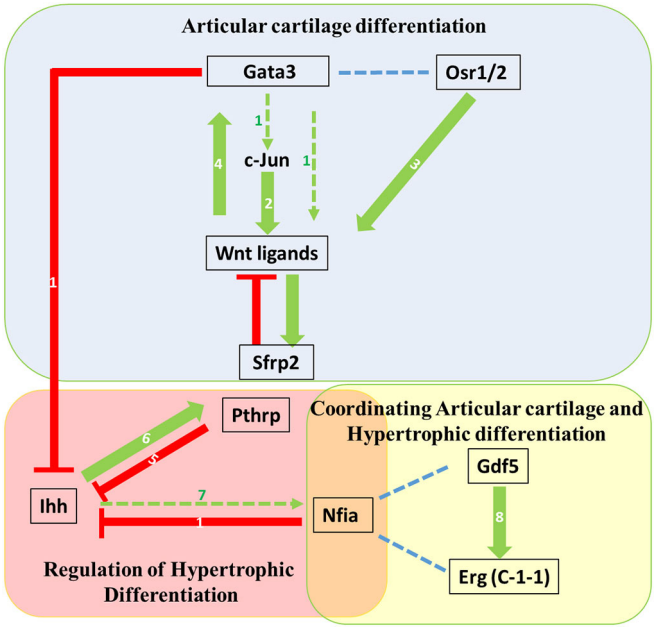

Fig. 8. Model of role of *Gata3* and *Nfia* in articular cartilage differentiation. Arrows with solid lines indicate demonstrated [either in this study (1) or in the published literature (2-8)] positive (green) or inhibitory (red) functional interactions, while arrows with dashed lines indicate predicted regulation. Dashed blue lines indicate possible functional interaction of an unspecified nature. The numbers indicate the source of information. 2, Kan and Tabin (2013); 3, Gao et al. (2011); 4, Grote et al. (2008); 5, Lanske et al. (1996); 6, Vortkamp et al. (1996); 7, Genovesi et al. (2013); 8, Iwamoto et al. (2007).

Role of GATA3 in joint development

Germline deletion of *Gata3* in mice results in embryonic lethality by the time joint development initiates in the limbs, precluding analysis of its role in articular cartilage differentiation (Pandolfi et al., 1995). A limb-specific knockout of *Gata3* needs to be generated. In the absence of such a mouse model, we took advantage of the chick embryonic system. We made several attempts to knockdown GATA3 by miRNA, as we did for NFIA, but without success. We thus generated the m*Gata3*-EnR construct, which serves as a dominant-negative form by repressing transcription of GATA3 downstream genes. Such a strategy has previously been used for Gata4 (Kamei et al., 2011). Infection with m*Gata3*-EnR in chicken limbs resulted in a spectrum of malformations, with some of the characteristics similar to those of *Gata3* knockout mice, such as pooling of blood, hemorrhages and smaller size of the limb elements (Pandolfi et al., 1995). It is interesting that both gain- and loss-of-function of GATA3 resulted in inhibition of certain joint formation. In this context, it should be noted that Macias et al. (1993) reported that application of retinoic acid (RA) in the interdigital mesenchyme resulted in inhibition of joint formation. It is known that many of the GATA factors, including Gata4/6, are transcribed in an RA-dependent manner (Arceci et al., 1993; Mauney et al., 2010). Thus, it would be interesting to investigate if RA can induce *Gata3* in early limb skeletal anlagen and whether that affects joint induction. We speculate that GATA3 loss-of-function induces an ectopic BMP signaling domain, thus eliminating a permissive environment for joint induction (Ray et al., 2015).

In the 50 kb genomic region upstream of the mouse and human *Gata3* genes, five conserved regions containing ten putative TCF/Lef binding sites were identified by bioinformatics analysis (Grote et al., 2008). Therefore, *Gata3* transcription is speculated to be regulated by Wnt signaling through β-catenin. Misexpression of *Wnt9a* or β-catenin in the limb results in ectopic expression of articular cartilage markers such as *Enpp2* (*Atx*) and *Sfrp2* (Hartmann and Tabin, 2001). Interestingly, we observed that expression of m*Gata3* promotes ectopic expression of *c-JUN*, *WNT9A* and β-catenin. This suggests that *GATA3* is not only downstream of Wnt/β-catenin signaling, but also maintains it in a feedback loop via c-*JUN*. Furthermore, since *c-Jun* is known to promote the expression of Wnt ligands (Kan and Tabin, 2013), ectopic expression of *Wnt9a* and β-catenin might be an indirect effect of *c-Jun* activation by Gata3. Moreover, we observed that although m*Gata3* could induce the ectopic expression of a few articular cartilage-specific genes, more articular cartilage-specific genes were ectopically expressed when a constitutively active version of GATA3 was expressed (m*Gata3*-VP16). Since VP16 fusion allows a transcription factor to activate transcription even in the absence of co-factors, we speculate that GATA3, in addition to activating expression of *c-JUN*, acts in conjunction with other transcription factors to promote articular cartilage differentiation.

Development (2018) 145, dev156554. doi:10.1242/dev.156554

We have routinely observed that GATA3 gain-of-function induces the ectopic expression of articular cartilage-specific genes only in the vicinity of the interzone and not in cells at a distance from it. This suggests that only these cells are competent, whereas the cells distant from the joint site are not competent, to upregulate the expression of articular cartilage-specific genes even upon the expression of constitutively activate m*Gata3*, further underscoring the importance of context and/or the presence of other transcription factors.

As of now, three transcription factors expressed in the joint interzone, namely the C-1-1 variant of *ERG*, *OSR1/2* and *c-JUN*, have been identified to play important roles during articular cartilage differentiation (Iwamoto et al., 2000, 2001, 2007; Gao et al., 2011; Kan and Tabin, 2013). C-1-1 misexpression prevents hypertrophic differentiation but does not promote ectopic expression of articular cartilage-specific genes other than tenascin C (Iwamoto et al., 2000, 2007). However, articular cartilage-specific ablation of *Erg* does not affect embryonic articular cartilage differentiation but leads to osteoarthritis-like phenotypic defects in 11-month-old mice (Ohta et al., 2015). c-Jun, presumably owing to its ability to promote transcription of the Wnt ligands *Wnt9a* and *Wnt16*, is necessary for articular cartilage differentiation (Kan and Tabin, 2013). However, as no gain-of-function study has been conducted, it is unclear if c-JUN is sufficient for articular cartilage differentiation. c-JUN loss-of-function spares specification of the interzone. *OSR1/2* compound knockout abrogates joint formation and promotes ectopic transient cartilage differentiation in the putative joint region (Gao et al., 2011). Nonetheless, since OSR1/2 loss-of-function reduces the expression of Wnt ligands and since β-catenin loss-of-function did not affect OSR1/2 expression, it is likely that OSR1/2 acts upstream of Wnt ligand expression and collaborates with transcriptional targets of the Wnt signaling pathway to promote articular cartilage differentiation (Gao et al., 2011). Since OSR1/2 misexpression studies have not been carried out, it is difficult to assess whether OSR1/2 can induce articular cartilage fate like GATA3. By conducting both loss- and gain-of-function analyses we have demonstrated that NFIA and GATA3 act at two different levels during articular cartilage differentiation. NFIA, similar to C-1-1, acts by preventing hypertrophic differentiation in the articular region, whereas GATA3 promotes articular cartilage fate by activating the expression of several articular cartilage-specific genes. However, to do this, GATA3 needs to collaborate with other transcription factors. It remains to be seen whether OSR1/2 and c-JUN are such transcription factors (Fig. 8).

Crosstalk between articular cartilage and transient cartilage differentiation

Gain- or loss-of-function of NFIA and gain-of-function of GATA3 affected not only articular cartilage differentiation but also hypertrophic differentiation, albeit at different levels. The role of an Ihh/Pthrp feedback loop in controlling hypertrophic differentiation is well established (Kronenberg, 2003). However, it is unlikely that these are the only two players involved in the process. Ihh loss-of-function causes absence of articular joints (St-Jacques et al., 1999; Koyama et al., 2007). This is unlikely to be due to the effect of Ihh on Pthrp expression, as Pthrp is not known to promote articular cartilage differentiation. Rather, it is probable that loss-of-function of Ihh is affecting some factor(s) that is directly or indirectly responsible for articular cartilage differentiation. Unfortunately, we could not find any data in the literature that describe changes in Ihh expression upon gain or loss of ERG function but, interestingly, loss of IHH does not cause loss of ERG variant C-1-1 expression (Koyama et al., 2007). In keeping with this, gain-of-function of C-1-1 blocks hypertrophic differentiation but does not affect articular cartilage differentiation, whereas NFIA gain-of-function not only blocks hypertrophic differentiation but also affects articular cartilage differentiation. In the context of medulla blastoma, *Ptch1* is reported to regulate *Nfia* expression (Genovesi et al., 2013). Thus, it is possible that NFIA is one of the regulators of the crosstalk between articular cartilage and hypertrophic cartilage differentiation. It is interesting to note that loss of GATA3 function did not affect hypertrophy, whereas loss of NFIA did. As NFIA and GATA3 seem to act at different stages of articular cartilage differentiation, it is possible that GATA3 loss-of-function blocks articular cartilage differentiation but does not affect expression of the factors that control hypertrophic differentiation, e.g. PTHrP and/or IHH. GATA3 gain-of-function did not affect NFIA expression (Fig. 6) but causes ectopic articular cartilage differentiation as well as block in hypertrophy. However, our data cannot rule out the possibility that these are two unconnected events. Unfortunately, we could not obtain any embryos in which m*Gata3*-VP16 was expressed only in hypertrophic cartilage and not in articular cartilage.

In summary, it appears that a network involving GATA3, OSR1/2, c-JUN and Wnt ligands regulates articular cartilage differentiation, that another network involving NFIA, GDF5 and ERG prevents transient cartilage differentiation in the articular cartilage domain, and that a third network involving IHH, PTHrP, NFIA and C-1-1 controls the crosstalk between articular cartilage differentiation and hypertrophy. The network that controls articular cartilage differentiation is becoming clearer. However, the mechanisms of action of the network that prevents ectopic hypertrophy in the articular cartilage domain and of that which controls crosstalk between articular cartilage and hypertrophic cells remain enigmatic. Our study provides potential new avenues for investigation into these aspects.

MATERIALS AND METHODS

Tissues

Fertilized White Leghorn chicken eggs were obtained from the Central Avian Research Institute of India, Chandra Shekhar Azad Agricultural University (Kanpur, UP, India) and Ganesh Enterprises (Nankari, Kanpur, UP, India). Eggs were incubated at 38°C in a humidified chamber to be treated and/or harvested at specific stages of development as assessed by Hamburger and Hamilton (HH) staging criteria (Hamburger and Hamilton, 1951).

Mouse experiments were conducted as per protocol approved by the Institute Animal Ethics Committee (registration number CPCSEA-56/1999). $Nfia^{-/+}$ male and female mice were mated, embryos were harvested at E16.5 and genotyped (das Neves et al., 1999) to identify $Nfia^{-/-}$ and wild type ($Nfia^{+/+}$).

Alcian Blue and Alizarin Red staining

Chicken embryos were harvested and eviscerated in PBS and fixed in 95% ethanol for at least 2-3 days, followed by overnight fixation in 100% acetone. Next, the tissues were stained for 2-3 days in a 1:1:1:17 volume mixture of 0.3% Alcian Blue 8GX (Sigma-Aldrich) in 95% ethanol:0.1% Alizarin Red in 70% ethanol:glacial acetic acid:70% ethanol. Post-staining, the tissues were cleared in 1% KOH and photographed under a dissection microscope.

Tissue processing

Chick embryonic limbs were dissected and fixed overnight in 4% paraformaldehyde (PFA) at 4°C, embedded in paraffin and 5-10 µm sections cut along the parasagittal plane using a microtome.

Development (2018) 145, dev156554. doi:10.1242/dev.156554

RNA *in situ* hybridization

cDNA clones used to make digoxigenin-labeled antisense riboprobes generated by *in vitro* transcription are detailed in Table S2. RNA *in situ* hybridization was performed as described previously (Singh et al., 2016). The RNA *in situ* hybridization signals for a given probe on control and test sections were developed on the same slide.

Immunohistochemistry

For pSMAD1/5/8, β-catenin, noggin and GFP immunohistochemistry, sections were processed and detected as described in Ray et al. (2015).

Immunohistochemistry

Sections were deparaffinized and rehydrated in PBS, followed by post-fixation in 4% PFA. Sections were incubated overnight at 4°C with the following primary antibodies: anti-pH3 (Sigma-Aldrich, H0412; 1:100), anti-β-catenin-Cy3 (Sigma-Aldrich, C7738; 1:200), anti-GAG (3C2; Potts et al., 1987), anti-pSMAD1/5/8 (Cell Signaling, 9511; 1:100) and anti-ColX (DSHB hybridoma product X-AC9, deposited by T. F Linsenmayer; 1:20). Following this step, tissues were washed in PBT (PBS containing 0.1% Tween 20) and incubated with the respective secondary antibodies, including: DyLight 549 AffiniPure goat anti-rabbit IgG (Jackson ImmunoResearch Laboratories, 111-505-003; 1:200) for anti-pSMAD1/5/8 and anti-pH3; Alexa Fluor 488-conjugated anti-mouse IgG (Jackson ImmunoResearch Laboratories, 115-545-003; 1:250) for 3C2; and DyLight 549-conjugated anti-mouse IgG (Jackson ImmunoResearch Laboratories, 115-505-003; 1:250) for anti-ColX. The tissues were counterstained with DAPI and mounted in VECTASHIELD antifade reagent (Vector Laboratories, H-1000).

EdU labeling

EdU (E10415, C10083, Invitrogen) labeling and detection were performed as previously described (Ray et al., 2015).

Viral expression

DF1 (Himly et al., 1998) chicken embryo fibroblast cells were checked to ensure they were free of contamination. Cells were transfected with the RCAS-HA-m*Nfia* construct obtained from Benjamin Deneen (Deneen et al., 2006). Virus particles were produced, concentrated and titered as described previously (Logan and Tabin, 1998). HH10 embryos were lowered within the egg by removing 2-3 ml of albumin and a window made through which a viral solution of titer 1×10^8 IU/ml mixed with 1% Fast Green was injected into the lateral plate mesoderm (LPM), which is destined to give rise to the prospective hindlimb of the embryo.

In ovo electroporation

Chick embryos were initially lowered by removing 2-3 ml of albumin and a window made to visualize the embryo under the vitelline membrane. This vitelline membrane was shorn near the hindlimb field and bathed in 100 µl sterile PBS+Pen Strep solution (Thermo Fisher Scientific, 10378016). At HH14, RCAS-HA-m*Nfia*, RCAS-cNFIA shRNAi (target region within *NFIA* coding sequence: 5′-GCCATCGCCAACTGCATTAAA-3′) obtained from Benjamin Deneen (Deneen et al., 2006), RCAS-GATA3-DBD-VP16 or RCAS-GATA3-DBD-EnR mixed with 0.5 µg/µl pCAG-mCherry and 0.1% Fast Green was injected into the embryonic space between the somatic LPM and splanchnic LPM at 2 µg/µl using a microinjector. Electroporation was performed as previously described (Suzuki and Ogura, 2008).

Acknowledgements

We are grateful to Prof. Andrew Lassar (Harvard Medical School, USA) for sharing full-length mouse GATA3 construct and to Prof. Benjamin Deneen (Baylor College of Medicine, Houston, TX, USA) for providing the RCAS-m*Nfia* and RCAS-cNFIA shRNAi constructs. We thank Prof. Richard Gronostajski for permission to obtain *Nfia* mutant mice from Prof. Shubha Tole.

Competing interests

The authors declare no competing or financial interests.

Author contributions

Conceptualization: P.N.P.S., A.B.; Methodology: P.N.P.S., A.B.; Validation: P.N.P.S., U.S.Y., A.B.; Formal analysis: P.N.P.S., U.S.Y., K.A., P.G.; Investigation: P.N.P.S., K.A., P.G.; Resources: V.K., A.B.; Data curation: P.N.P.S., U.S.Y.; Writing - original draft: P.N.P.S., A.B.; Writing - review & editing: P.N.P.S., U.S.Y., A.B.; Visualization: P.N.P.S., U.S.Y., A.B.; Supervision: A.B.; Project administration: A.B.; Funding acquisition: A.B.

Funding

This work was supported by grants from the Department of Biotechnology, Ministry of Science and Technology, India (DBT) (BT/PR11202/MED/32/46/2008) and from the Science and Engineering Research Board of the Department of Science and Technology, Government of India (EMR/2015/001519 to A.B.). P.N.P.S. was supported by a fellowship from the Council of Scientific and Industrial Research (CSIR), India. U.S.Y. and K.A. were supported by fellowships from the Ministry of Human Resource Development (MHRD), India and V.K. was supported by a University Grants Commission (UGC) fellowship, India.

Supplementary information

Supplementary information available online at
http://dev.biologists.org/lookup/doi/10.1242/dev.156554.supplemental

References

Arceci, R. J., King, A. A., Simon, M. C., Orkin, S. H. and Wilson, D. B. (1993). Mouse GATA-4: a retinoic acid-inducible GATA-binding transcription factor expressed in endodermally derived tissues and heart. *Mol. Cell. Biol.* **13**, 2235-2246.

Archer, C. W., Dowthwaite, G. P. and Francis-West, P. (2003). Development of synovial joints. *Birth Defects Res. C Embryo Today* **69**, 144-155.

Bi, W., Deng, J. M., Zhang, Z., Behringer, R. R. and de Crombrugghe, B. (1999). Sox9 is required for cartilage formation. *Nat. Genet.* **22**, 85-89.

Bonilla-Claudio, M., Wang, J., Bai, Y., Klysik, E., Selever, J. and Martin, J. F. (2012). Bmp signaling regulates a dose-dependent transcriptional program to control facial skeletal development. *Development* **139**, 709-719.

das Neves, L., Duchala, C. S., Tolentino-Silva, F., Haxhiu, M. A., Colmenares, C., Macklin, W. B., Campbell, C. E., Butz, K. G. and Gronostajski, R. M. (1999). Disruption of the murine nuclear factor I-A gene (Nfia) results in perinatal lethality, hydrocephalus, and agenesis of the corpus callosum. *Proc. Natl. Acad. Sci. USA* **96**, 11946-11951.

Deneen, B., Ho, R., Lukaszewicz, A., Hochstim, C. J., Gronostajski, R. M. and Anderson, D. J. (2006). The transcription factor NFIA controls the onset of gliogenesis in the developing spinal cord. *Neuron* **52**, 953-968.

Dentice, M., Bandyopadhyay, A., Gereben, B., Callebaut, I., Christoffolete, M. A., Kim, B. W., Nissim, S., Mornon, J.-P., Zavacki, A. M., Zeöld, A. et al. (2005). The Hedgehog-inducible ubiquitin ligase subunit WSB-1 modulates thyroid hormone activation and PTHrP secretion in the developing growth plate. *Nat. Cell Biol.* **7**, 698-705.

Francis-West, P. H., Abdelfattah, A., Chen, P., Allen, C., Parish, J., Ladher, R., Allen, S., MacPherson, S., Luyten, F. P. and Archer, C. W. (1999). Mechanisms of GDF-5 action during skeletal development. *Development* **126**, 1305-1315.

Gao, Y., Lan, Y., Liu, H. and Jiang, R. (2011). The zinc finger transcription factors Osr1 and Osr2 control synovial joint formation. *Dev. Biol.* **352**, 83-91.

Genovesi, L. A., Ng, C. G., Davis, M. J., Remke, M., Taylor, M. D., Adams, D. J., Rust, A. G., Ward, J. M., Ban, K. H., Jenkins, N. A. et al. (2013). Sleeping Beauty mutagenesis in a mouse medulloblastoma model defines networks that discriminate between human molecular subgroups. *Proc. Natl. Acad. Sci. USA* **110**, E4325-E4334.

Grote, D., Boualia, S. K., Souabni, A., Merkel, C., Chi, X., Costantini, F., Carroll, T. and Bouchard, M. (2008). Gata3 acts downstream of beta-catenin signaling to prevent ectopic metanephric kidney induction. *PLoS Genet.* **4**, e1000316.

Guo, X., Day, T. F., Jiang, X., Garrett-Beal, L., Topol, L. and Yang, Y. (2004). Wnt/beta-catenin signaling is sufficient and necessary for synovial joint formation. *Genes Dev.* **18**, 2404-2417.

Hamburger, V. and Hamilton, H. L. (1951). A series of normal stages in the development of the chick embryo. *J. Morphol.* **88**, 49-92.

Hartmann, C. and Tabin, C. J. (2001). Wnt-14 plays a pivotal role in inducing synovial joint formation in the developing appendicular skeleton. *Cell* **104**, 341-351.

Himly, M., Foster, D. N., Bottoli, I., Iacovoni, J. S. and Vogt, P. K. (1998). The DF-1 chicken fibroblast cell line: transformation induced by diverse oncogenes and cell death resulting from infection by avian leukosis viruses. *Virology* **248**, 295-304.

Holder, N. (1977). An experimental investigation into the early development of the chick elbow joint. *J. Embryol. Exp. Morphol.* **39**, 115-127.

Iwamoto, M., Higuchi, Y., Koyama, E., Enomoto-Iwamoto, M., Kurisu, K., Yeh, H., Abrams, W. R., Rosenbloom, J. and Pacifici, M. (2000). Transcription factor ERG variants and functional diversification of chondrocytes during limb long bone development. *J. Cell Biol.* **150**, 27-40.

Iwamoto, M., Higuchi, Y., Enomoto-Iwamoto, M., Kurisu, K., Koyama, E., Yeh, H., Rosenbloom, J. and Pacifici, M. (2001). The role of ERG (ets related gene) in cartilage development. *Osteoarthritis Cartilage* **9** Suppl. A, S41-S47.

Iwamoto, M., Tamamura, Y., Koyama, E., Komori, T., Takeshita, N., Williams, J. A., Nakamura, T., Enomoto-Iwamoto, M. and Pacifici, M. (2007). Transcription factor ERG and joint and articular cartilage formation during mouse limb and spine skeletogenesis. *Dev. Biol.* **305**, 40-51.

Kamei, C. N., Kempf, H., Yelin, R., Daoud, G., James, R. G., Lassar, A. B., Tabin, C. J. and Schultheiss, T. M. (2011). Promotion of avian endothelial cell differentiation by GATA transcription factors. *Dev. Biol.* **353**, 29-37.

Kan, A. and Tabin, C. J. (2013). c-Jun is required for the specification of joint cell fates. *Genes Dev.* **27**, 514-524.

Karsenty, G. and Wagner, E. F. (2002). Reaching a genetic and molecular understanding of skeletal development. *Dev. Cell* **2**, 389-406.

Kouros-Mehr, H., Slorach, E. M., Sternlicht, M. D. and Werb, Z. (2006). GATA-3 maintains the differentiation of the luminal cell fate in the mammary gland. *Cell* **127**, 1041-1055.

Koyama, E., Ochiai, T., Rountree, R. B., Kingsley, D. M., Enomoto-Iwamoto, M., Iwamoto, M. and Pacifici, M. (2007). Synovial joint formation during mouse limb skeletogenesis: roles of Indian hedgehog signaling. *Ann. N. Y. Acad. Sci.* **1116**, 100-112.

Koziel, L., Wuelling, M., Schneider, S. and Vortkamp, A. (2005). Gli3 acts as a repressor downstream of Ihh in regulating two distinct steps of chondrocyte differentiation. *Development* **132**, 5249-5260.

Kronenberg, H. M. (2003). Developmental regulation of the growth plate. *Nature* **423**, 332-336.

Lanske, B., Karaplis, A. C., Lee, K., Luz, A., Vortkamp, A., Pirro, A., Karperien, M., Defize, L. H., Ho, C., Mulligan, R. C. et al. (1996). PTH/PTHrP receptor in early development and Indian hedgehog-regulated bone growth. *Science* **273**, 663-666.

Logan, M. and Tabin, C. (1998). Targeted gene misexpression in chick limb buds using avian replication-competent retroviruses. *Methods* **14**, 407-420.

Macias, D., Ganan, Y. and Hurle, J. M. (1993). Modification of the phalangeal pattern of the digits in the chick embryo leg bud by local microinjection of RA, staurosporin and TGF beta. *Anat. Embryol. (Berl)* **188**, 201-208.

Mauney, J. R., Ramachandran, A., Richard, N. Y., Daley, G. Q., Adam, R. M. and Estrada, C. R. (2010). All-trans retinoic acid directs urothelial specification of murine embryonic stem cells via GATA4/6 signaling mechanisms. *PLoS ONE* **5**, e11513.

Merino, R., Macias, D., Gañan, Y., Economides, A. N., Wang, X., Wu, Q., Stahl, N., Sampath, K. T., Varona, P. and Hurle, J. M. (1999). Expression and function of Gdf-5 during digit skeletogenesis in the embryonic chick leg bud. *Dev. Biol.* **206**, 33-45.

Ohta, Y., Okabe, T., Larmour, C., Di Rocco, A., Maijenburg, M. W., Phillips, A., Speck, N. A., Wakitani, S., Nakamura, T., Yamada, Y. et al. (2015). Articular cartilage endurance and resistance to osteoarthritic changes require transcription factor Erg. *Arthritis Rheumatol.* **67**, 2679-2690.

Pacifici, M., Koyama, E. and Iwamoto, M. (2005). Mechanisms of synovial joint and articular cartilage formation: recent advances, but many lingering mysteries. *Birth Defects Res. C Embryo Today* **75**, 237-248.

Pandolfi, P. P., Roth, M. E., Karis, A., Leonard, M. W., Dzierzak, E., Grosveld, F. G., Engel, J. D. and Lindenbaum, M. H. (1995). Targeted disruption of the GATA3 gene causes severe abnormalities in the nervous system and in fetal liver haematopoiesis. *Nat. Genet.* **11**, 40-44.

Pitsillides, A. A. and Beier, F. (2011). Cartilage biology in osteoarthritis–lessons from developmental biology. *Nat. Rev. Rheumatol.* **7**, 654-663.

Potts, W. M., Olsen, M., Boettiger, D. and Vogt, V. M. (1987). Epitope mapping of monoclonal antibodies to gag protein p19 of avian sarcoma and leukaemia viruses. *J. Gene. Virol.* **68**, 3177-3182.

Ray, A., Singh, P. N. P., Sohaskey, M. L., Harland, R. M. and Bandyopadhyay, A. (2015). Precise spatial restriction of BMP signaling is essential for articular cartilage differentiation. *Development* **142**, 1169-1179.

Shubin, N. H. and Alberch, P. (1986). A morphogenetic approach to the origin and basic organization of the tetrapod limb. *Evol. Biol.* **20**, 319-387.

Singh, P. N. P., Ray, A., Azad, K. and Bandyopadhyay, A. (2016). A comprehensive mRNA expression analysis of developing chicken articular cartilage. *Gene Expr. Patterns* **20**, 22-31.

Später, D., Hill, T. P., Gruber, M. and Hartmann, C. (2006a). Role of canonical Wnt-signalling in joint formation. *Eur. Cell Mater.* **12**, 71-80.

Später, D., Hill, T. P., O'Sullivan, R. J., Gruber, M., Conner, D. A. and Hartmann, C. (2006b). Wnt9a signaling is required for joint integrity and regulation of Ihh during chondrogenesis. *Development* **133**, 3039-3049.

St-Jacques, B., Hammerschmidt, M. and McMahon, A. P. (1999). Indian hedgehog signaling regulates proliferation and differentiation of chondrocytes and is essential for bone formation. *Genes Dev.* **13**, 2072-2086.

Storm, E. E. and Kingsley, D. M. (1999). GDF5 coordinates bone and joint formation during digit development. *Dev. Biol.* **209**, 11-27.

Suzuki, T. and Ogura, T. (2008). Congenic method in the chick limb buds by electroporation. *Dev. Growth Differ.* **50**, 459-465.

Tsumaki, N., Tanaka, K., Arikawa-Hirasawa, E., Nakase, T., Kimura, T., Thomas, J. T., Ochi, T., Luyten, F. P. and Yamada, Y. (1999). Role of CDMP-1 in skeletal morphogenesis: promotion of mesenchymal cell recruitment and chondrocyte differentiation. *J. Cell Biol.* **144**, 161-173.

Vortkamp, A., Lee, K., Lanske, B., Segre, G. V., Kronenberg, H. M. and Tabin, C. J. (1996). Regulation of rate of cartilage differentiation by Indian hedgehog and PTH-related protein. *Science* **273**, 613-622.